Received: 16 June 2022 | First decision: 7 August 2022 | Accepted: 7 December 2022

DOI: 10.1111/apt.17363

AP&T Alimentary Pharmacology & Therapeutics WILEY

Machine learning liver histology scores correlate with portal hypertension assessments in nonalcoholic steatohepatitis cirrhosis

Mazen Noureddin[1] | Zachary Goodman[2] | Dean Tai[3] | Elaine L. K. Chng[3] | Yayun Ren[3] | Pol Boudes[4] | Harold Shlevin[4] | Guadalupe Garcia-Tsao[5] | Stephen A. Harrison[6] | Naga P. Chalasani[7]

[1]Houston Methodist Hospital and Houston Research Institute, Houston, Texas, USA

[2]Inova Fairfax Hospital, Falls Church, Virginia, USA

[3]HistoIndex Pte. Ltd., Singapore, Singapore

[4]Galectin Therapeutics Inc., Norcross, USA

[5]Section of Digestive Diseases, Yale University and CT-VA Healthcare System, New Haven, Connecticut, USA

[6]Pinnacle Clinical Research, San Antonio, Texas, USA

[7]Division of Gastroenterology and Hepatology, Department of Medicine, Indiana University School of Medicine, Indianapolis, Indiana, USA

Correspondence
Mazen Noureddin, 8900 Beverly Blvd., Los Angeles, CA 90048, USA.
Email: mazen.noureddin@cshs.org

Funding information
Galectin Therapeutics Inc

Summary

Background and Aims: In cirrhotic nonalcoholic steatohepatitis (NASH) clinical trials, primary efficacy endpoints have been hepatic venous pressure gradient (HVPG), liver histology and clinical liver outcomes. Important histologic features, such as septa thickness, nodules features and fibrosis area have not been included in the histologic assessment and may have important clinical relevance. We assessed these features with a machine learning (ML) model.

Methods: NASH patients with compensated cirrhosis and HVPG ≥6 mm Hg ($n = 143$) from the Belapectin phase 2b trial were studied. Liver biopsies, HVPG measurements and upper endoscopies were performed at baseline and at end of treatment (EOT). A second harmonic generation/two-photon excitation fluorescence provided an automated quantitative assessment of septa, nodules and fibrosis (SNOF). We created ML scores and tested their association with HVPG, clinically significant HVPG (≥10 mm Hg) and the presence of varices (SNOF-V).

Results: We derived 448 histologic variables (243 related to septa, 21 related to nodules and 184 related to fibrosis). The SNOF score (≥11.78) reliably distinguished CSPH at baseline and in the validation cohort (baseline + EOT) [AUC = 0.85 and 0.74, respectively]. The SNOF-V score (≥0.57) distinguished the presence of varices at baseline and in the same validation cohort [AUC = 0.86 and 0.73, respectively]. Finally, the SNOF-C score differentiated those who had >20% change in HVPG against those who did not, with an AUROC of 0.89.

Conclusion: The ML algorithm accurately predicted HVPG, CSPH, the development of varices and HVPG changes in patients with NASH cirrhosis. The use of ML histology model in NASH cirrhosis trials may improve the assessment of key outcome changes.

Mazen Noureddin and Naga P. Chalasani contributed equally.

The Handling Editor for this article was Professor Grace Wong, and it was accepted for publication after full perr-review.

1 | INTRODUCTION

Nonalcoholic fatty liver disease (NAFLD) can progress to nonalcoholic steatohepatitis (NASH), which has become the leading cause of cirrhosis overall, the leading cause of liver transplantation in women, and the second leading cause of liver transplantation in men.[1,2] Emerging therapies are being examined to treat NASH patients, including those with cirrhosis.[3-5] However, treating cirrhotic patients is complex since quantification of fibrosis is challenging and has been inadequately studied in NASH cirrhosis. Nevertheless, evidence from cirrhosis of other causes, such as chronic hepatitis B and C, suggest that measurement of fibrosis regression is a goal within reach and has opened the door for the development of drugs that target fibrosis (e.g., antifibrotics).[6,7]

Recent efforts have determined NASH aetiology as a cause of cirrhosis and have defined the primary efficacy end points in trials of NASH cirrhosis.[8,9] Defining the end points has proven challenging, however, because of the lack of data on the natural history and of drugs effective in reversing cirrhosis. Historical evidence has led to using hepatic portal pressure gradient (HVPG) in NASH cirrhosis trials as a primary end point, especially in patients with elevated HVPG.[10,11] This approach was supported by evidence from cirrhosis of other causes that HVPG correlates with clinical liver events,[12] and improvement of HVPG is associated with clinical benefits. However, the use of HVPG is challenging in NASH cirrhosis trials because this technique is limited to expert academic centres, variabilities in reading in NASH cirrhosis patients, cost and invasiveness of the procedure, and patients' acceptance.[13] Thus, one-stage improvement of fibrosis in NASH cirrhosis patients, especially those with compensated cirrhosis, has been proposed as an alternative to HVPG measurements.[14] Although linear improvement of fibrosis has correlated with improvement in clinical liver events,[15] this assessment has limitations as well: it ignores other important architectural changes in cirrhosis, including the extent of fibrosis area, septal thickness and size and numbers of nodules.[16] Studies from hepatitis C, using semi-quantitative methods, have found that considering these features can be helpful in accurately correlating histology with portal pressure in cirrhotic patients[17-19]; however, these semi-quantitative techniques have limited the use of that novel concept, as readings are prone to variabilities.

The emergence of machine learning (ML) technology in reading liver histology has advanced the field and limited inter- and intra-observer variabilities.[20,21] A recent study from a NASH cirrhosis clinical trial has found that a machine learning-based model on trichrome-stained liver biopsy slides can predict clinically significant portal hypertension (CSPH) in NASH cirrhosis patients.[22] However, nodule size was weakly correlated with HVPG in this model, while septa thickness was not considered.[22]

Here, we developed 448 histologic variables to develop a ML model for correlation with HVPG. We hypothesised that our model would correlate with HVPG and the presence of oesophageal varices assessed in a phase 2 clinical trial that examined the efficacy of belapectin, an inhibitor of galectin 3, in patients with NASH cirrhosis and portal hypertension.[10]

2 | MATERIALS AND METHODS

2.1 | Study cohort

The study was approved by the institutional review board of the participating sites and has been described in detail.[10] Patients with NASH cirrhosis and portal hypertension (HVPG ≥6 mm Hg), enrolled from 36 centres, were randomised to 52 weeks of treatment with belapectin 2 or 8 mg/kg or placebo. Patients received upper endoscopy within 2 months before randomisation and within 14–28 days after the final dose of the experimental drug. Varices were classified as small, medium or large.[10]

2.2 | HVPG measurements and liver histology

HVPG measurements were performed at each site. Before the start of the study, each site underwent evaluation of their HVPG technique, and passed quality assessment by an expert HVPG central reader. HVPG were performed by advancing a balloon catheter into the hepatic vein under fluoroscopic guidance. Free hepatic pressure was measured when the balloon was completely deflated; wedge pressure was measured upon inflation of the balloon and occlusion of the hepatic vein. Three measurements of the hepatic vein and wedge pressure were obtained and transmitted to the central reader. Liver biopsies of mean length of 2.5 cm were obtained.[23] Liver histology was read by an expert liver pathologist central reader. Steatohepatitis was assessed according to Brunt criteria[24]; the NASH activity score, graded according to the NASH clinical research network,[25] was used to semi-quantify the cellular activity; fibrosis was assessed according to the Ishak score and the NASH clinical research network score.

2.3 | Image acquisition

The images of 286 unstained slides from 143 patients were acquired by use of a second harmonic generation/two-photon excitation fluorescence (SHG/TPE) imaging system (Genesis™ system, HistoIndex Pte. Ltd.). Histoindex was blinded to the assigned treatment group (reported elsewhere),[10] HVPG and endoscopies results upon receiving the slides and until the end of the histological analysis process. The collagen and histologic structures were visualised by SHG microscopy and TPE microscopy, respectively. Details of the procedure have been described elsewhere.[23] Image tiles were acquired at 20x objective with 512 × 512 pixels resolution with a dimension of 200 × 200 μm.[2] Multiple adjacent tiles were captured to encompass the whole tissue area in each needle biopsy.

2.4 | Image quantification

The initial algorithm version developed for septa detection was based on a hepatitis B virus (HBV) patient cohort using SHG/TPEF

imaging technology.[26] The algorithm is further refined by using an expert pathologist's septa annotations on 25 digitised NASH slides stained with picrosirius red, and immunostain for smooth muscle actin. In addition to annotating for septa, cirrhotic nodules were also annotated and these annotations were used to develop a separate algorithm for nodule detection.

The SHG/TPE images of unstained slides were analysed with a digital image processing algorithm that can quantify (1) 243 *septa* criteria, including the morphological characteristics of septa, such as area, length and width, and the collagen and cellular regions inside the region of septa; (2) 21 *nodule* criteria, such as number of nodules and length of nodules; (3) 184 *fibrosis* criteria in various regions in liver tissue, including the portal-septa, peri-septal, mid-nodular, peri-venular and hepatic venule regions. In total, 448 criteria were quantified by the image processing algorithm based on Matlab 2015a (MathWorks, Inc.).

Using this ML model, fibrosis was quantified in regions that are specific only to cirrhotic samples. In these cirrhotic samples, the portal tract areas were observed to coincide with septa, and we termed these regions "portal-septal". Centrilobular and peri-portal regions can be difficult to visualise in a cirrhotic liver, but lineage markers such as glutamine synthetase have shown that the peri-septal hepatocyte cells are derived from the centrilobular cells of a normal liver.[27] Given that the peri-portal regions are observed near the septa in these cirrhotic samples, it is designated as "peri-septal". Further, the centrilobular region surrounding central veins in a normal liver does not apply in a cirrhotic nodule, and since the central vein is a tributary of the hepatic vein, peri-central is renamed as "peri-venular" and central vein as "hepatic venule". Lastly, the rest of the parenchyma (Zone 2) of the nodules consists of some regenerative nodules, so we have termed as "mid-nodular" for the purpose of this analysis. The definitions of these regions are illustrated in Figure 1.

Using SHG/TPE, the visualisation of these fibrosis in these regions, as well as septa and nodules were shown. (Figure 2) Using the ML model, 18 septa (Figure 2A) and 19 nodules (Figure 2B) were detected while fibrosis (Figure 2C) was quantified in the regions as described above.

2.5 | Model construction

The training and validation work flows to establish the ML models are summarised in Figure 3. To assess the HVPG for patients, septa, nodules and fibrosis criteria from the baseline cohort were used for building single scores which were septa-only, nodule-only and fibrosis-only scores, respectively.

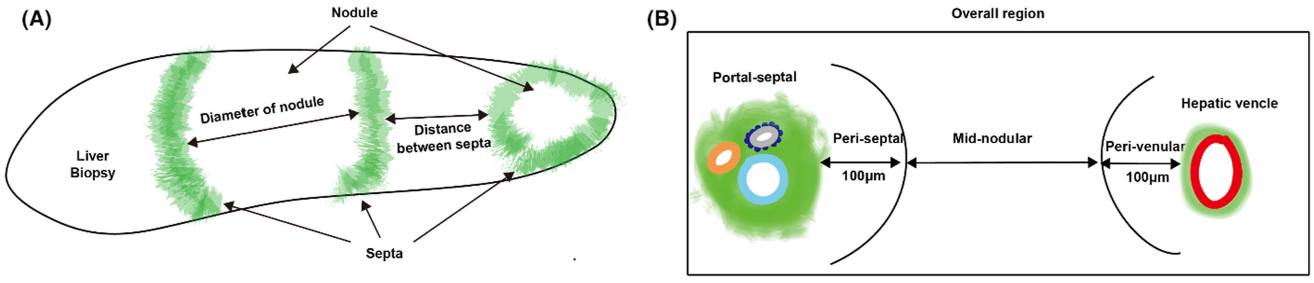

FIGURE 1 (A) An illustrative example of a liver biopsy showing septa, nodules, diameter of nodule and distance between septa as defined by the algorithm. (B) An illustrative example showing the five regions in which fibrosis is quantified by the algorithm: the portal-septa, peri-septal, mid-nodular, peri-venular and hepatic venule.

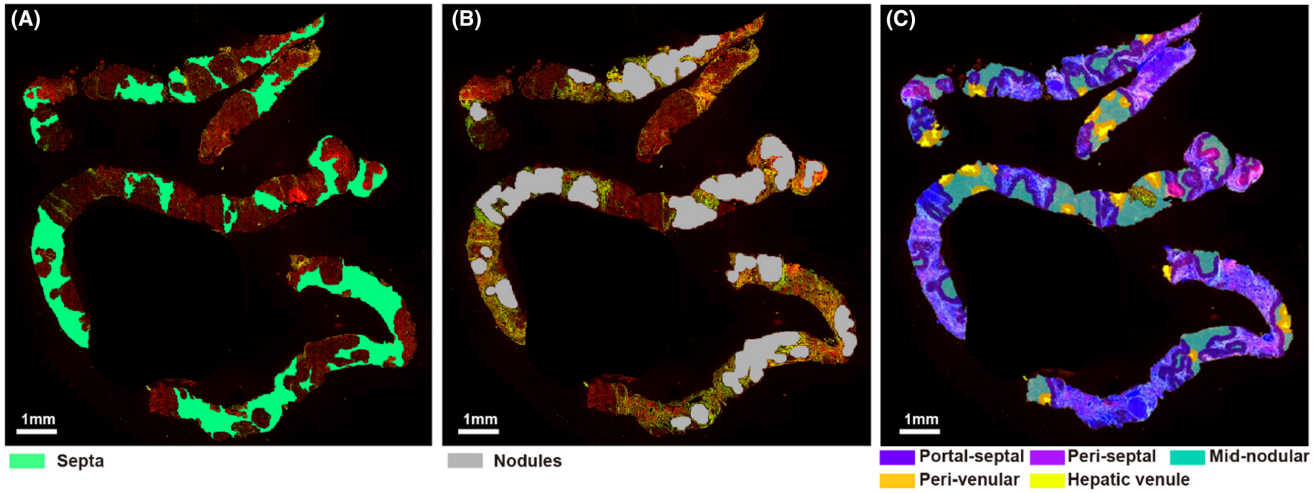

FIGURE 2 SHG/TPE image showing the AI annotations of (A) septa, (B) nodules and (C) fibrosis as analysed in the portal-septal and peri-septal regions

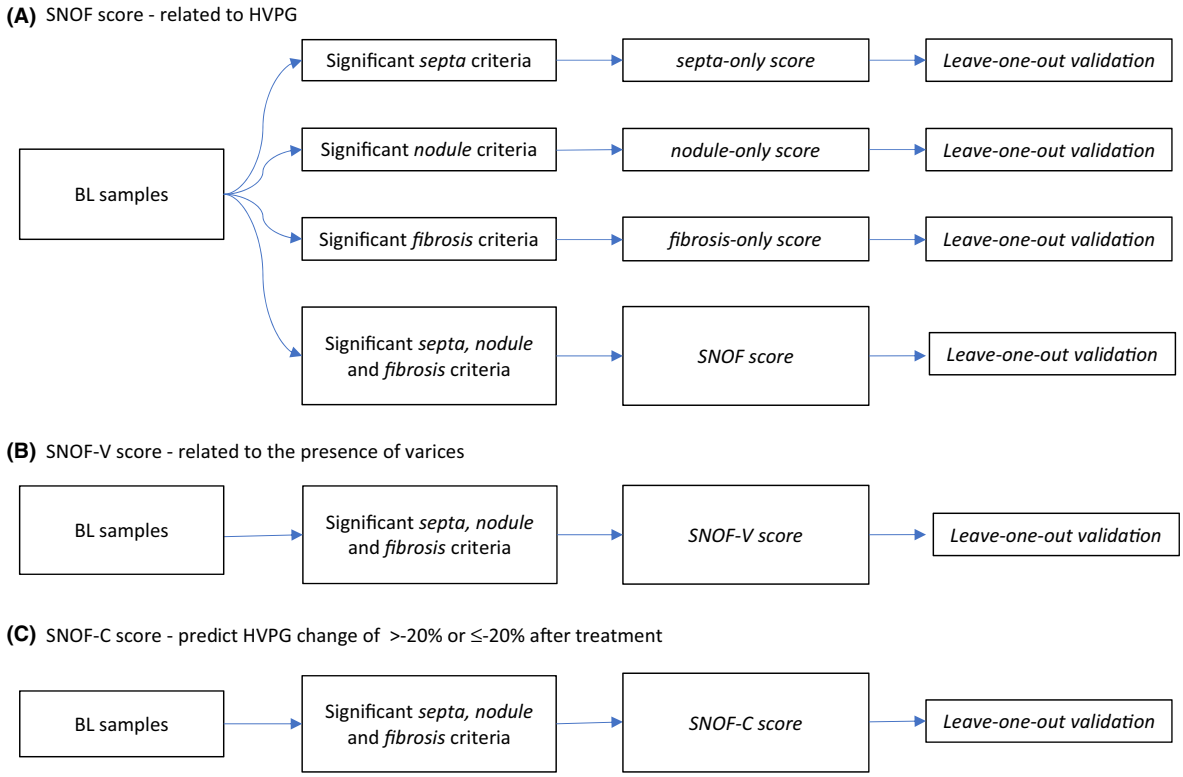

FIGURE 3 Training and validation workflows for (A) SNOF, (B) SNOF-V and (C) SNOF-C scores

In addition to building ML models with parameters based on a single histological feature, the septa, nodules and fibrosis parameters were also combined to build three models designated as (A) SNOF score that related to HVPG, (B) SNOF-V score that related to the presence or development of varices and (C) SNOF-C score that is related to HVPG change of >20% or ≤20% between baseline and end of treatment regardless of the treatment arm. Baseline liver biopsies were used as the training set for these models. With a sequential feature selection method, three sets of 15 parameters each were selected from the 448 parameters for the SNOF score, SNOF-V score and SNOF-C score, respectively. The distribution of these 15 parameters between the septa, nodules and fibrosis categories for the SNOF, SNOF-V and SNOF-C scores are provided in the Supplementary section (Tables S1–S3). The models were validated using the leave-one-out cross-validation method, which is a well-accepted validation method as previously reported.[28]

2.6 | Statistical analysis

The Spearman non-parametric method was used to estimate the correlation between SNOF score and HVPG. The difference in SNOF-V score between varices YES and NO samples was estimated by the Wilcoxon rank sum test. The area under the receiver operating characteristic curve (AUROC) analysis was performed to evaluate the performance of SNOF and SNOF-V scores. The cutoff values of SNOF score for evaluating the presence of significant portal hypertension, the cutoff values of SNOF-V score and the cutoff value for HVPG value for evaluating the presence of oesophageal varices, were determined with Youden's index. The sensitivity, specificity, negative predictive value (NPV) and positive predictive value (PPV), determined by the cutoff values, were calculated. Statistical significance level was set at $p < 0.05$. Statistical analyses were performed with Matlab 2015a (MathWorks, Inc., Natick, MA).

3 | RESULTS

3.1 | Detection of septa, nodules and fibrosis (SNOF)

The ML model identifies septa, nodules and fibrosis in the biopsy sample and quantifies their morphological features automatically. A total of 243 septa-related, 21 nodule-related and 184 fibrosis-related morphological features were analysed for each biopsy sample.

3.2 | Correlation of the SNOF ML model with HVPG

We assessed the degree of correlation among the septa-, nodules- and fibrosis-selected criteria on baseline biopsies, using them as training cohort, and we used the same biopsies as validation cohort by leaving one sample out. The results were consistent across the training cohorts and the validation cohorts (Table 1).

Next, a machine learning SNOF score was built by selecting the 15 best morphological parameters that correlated significantly with HVPG measurement (Tables S1 and S2) from each morphological feature described. The correlation of training and validation results of SNOF scores with HVPG is shown in Figure 3, with an r value of 0.67 in the training cohort and 0.57 in the leave-one-out validation. The combination of septa, nodules and fibrosis (SNOF) in an index outperforms using just septa, or nodule, or fibrosis separately (Table 1).

3.3 | Correlation of the SNOF ML model with presence of varices

We next created SNOF-varices (SNOF-V) scores by correlating variables with the presence of varices and selected the 15 best-correlated parameters for the final model. The performance of the SNOF-V score to distinguish the presence of oesophageal varices at baseline (pre-treatment) is shown in Figure 4.

TABLE 1 Summary of the correlation results among septa, nodules and fibrosis selected parameters when baseline biopsies were used as the training cohort. Correlation of SNOF score built by selecting 15 septa, nodules and fibrosis parameters is also shown

Parameters	Correlation results (*r* value)	
	Training using baseline samples	Leave-one-out validation
Septa only	0.55	0.44
Nodule only	0.52	0.39
Fibrosis only	0.57	0.44
SNOF	0.67	0.57

3.4 | Performances of SNOF score and SNOF-V scores

An optimum cutoff value of 11.78 was determined by correlating SNOF scores with HVPG value of ≥10 (CSPH). With this cutoff value, the performance of SNOF score in predicting HVPG ≥10 is summarised in Table 2. Similarly, the performance of SNOF-V score in predicting the presence of varices is also summarised in Table 2. The performance in predicting the presence of varices with an HVPG cutoff value at ≥10 is also included in the table as a reference. We validated the results by combining the baseline and end of treatment samples (Figure 5).

3.5 | Performance of SNOF-C in detecting clinically meaningful HVPG changes

We then divided the patients into those who had HVPG change of >20% or ≤20% between baseline and end of treatment regardless of the treatment arm. The SNOF-Change (SNOF-C) score was built based on the top 15 significant parameters that correlated with 20% changes in HVPG (Table S3). The SNOF-C score performed well in differentiating those who had >20% change in HVPG versus those who did not, with AUROC of 0.89 in the training Cohort and 0.79 in the validation cohort (Table 3). The performance criteria of SNOF-C score including sensitivity, specificity, PPV and NPV are shown in Table 3.

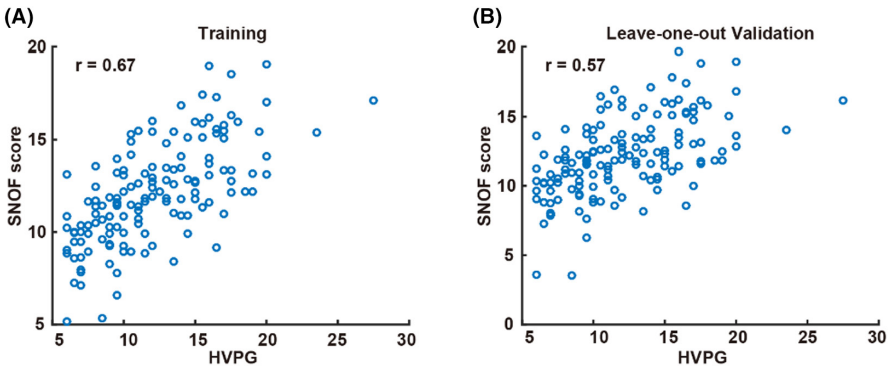

FIGURE 4 Scatter plots for the SNOF score. (A) Training using baseline samples and (B) validation using the leave-one-out method

TABLE 2 Summary of the performances of SNOF score and SNOF-varices (SNOF-V) scores at predicting HVPG and presence of varices, respectively

	Baseline					Baseline and end-of-treatment				
	AUC	Sensitivity	Specificity	PPV	NPV	AUC	Sensitivity	Specificity	PPV	NPV
SNOF score ≥11.78 to predict HVPG ≥10 (CSPH)	0.85	73%	86%	91%	62%	0.74	65%	76%	83%	54%
SNOF-V score ≥0.57 to predict varices	0.86	77%	86%	85%	78%	0.73	64%	78%	74%	70%
HVPG ≥10 to predict varices	0.75	84%	53%	65%	76%	0.74	82%	52%	62%	76%

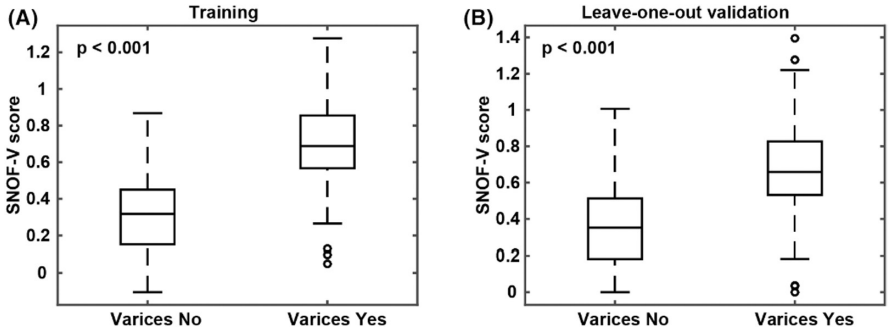

FIGURE 5 Boxplots for the SNOF-V score. (A) Training using baseline samples and (B) validation using the leave-one-out method

TABLE 3 Summary of the performances of SNOF-C score at predicting HVPG changes ≤ −20%

	Training					Leave-one-out validation				
	AUC	Sensitivity	Specificity	PPV	NPV	AUC	Sensitivity	Specificity	PPV	NPV
SNOF-C score >0.257 to predict HVPG changes ≤−20%	0.89	97%	69%	50%	99%	0.79	75%	63%	40%	89%

4 | DISCUSSION

The major outcome of this study was that the ML algorithm accurately extrapolated HVPG, CSPH and its changes, and the development of varices from liver histology in patients with NASH cirrhosis. Using the SHG/TPE machine learning model on baseline and end-of-treatment liver biopsies from the phase 2b belapectin trial in NASH cirrhosis patients,[10] we created 448 histologic variables related to key cirrhosis architectural features: septa, nodules and fibrosis. The slides from which the images were obtained were examined in a blinded manner. We then combined these features in various scores: one to assess correlation with HVPG (SNOF), one to distinguish the presence of varices (SNOF-V), and one to assess clinically meaningful changes of HVPG (SNOF-C). These scores performed well and can potentially be implemented in NASH cirrhosis clinical trials (without the need for measuring HVPG) to assess key changes in patients with cirrhosis. The use of ML histologic features and scores may increase the accuracy of the efficacy endpoints in cirrhotic NASH trials.

Given that patients with cirrhosis are at a much higher risk for decompensation and mortality, more screening measures have been developed to identify the right patient population for enrolment into cirrhotic NASH trials, including a recent surrogate score, the nonalcoholic fatty liver disease cirrhosis score (NCS), developed by Labenz et al which enables the differentiation of bridging fibrosis from cirrhosis.[29] Previous studies[17-19] have proposed subclassification of cirrhosis based on unique histologic features: septal width and thickness, numbers of nodules and nodule size. These studies were mainly done with small cohorts (<50 patients in two series) and did not include NASH cirrhosis as a cause. In a cohort of 43 patients, Nagula et al[17] found that small nodularity and thick fibrous septa were the only variables independently predictive of CSPH (HVPG ≥10 mm Hg), which is predictive of the development of complications of cirrhosis, including death. The authors used a semi-quantitative method to evaluate liver biopsies. Those findings were confirmed in a study conducted with patients who had cirrhosis mainly caused by hepatitis B.[19] These studies led to a position paper,[16] calling for pathophysiological classification of cirrhosis. In a subsequent study of 43 patients that used a quantitative methodology based on digital image analysis, total fibrosis area and small nodule size were both independently predictive of the presence of CSPH; septal width was not predictive.[18] The authors attributed the differences in findings of the two studies to differences in techniques used (semi-quantitative vs quantitative).[18] It appears that compensated cirrhosis might be classified into subcategories reflecting various degrees of severity, which is a crucial consideration when developing antifibrotic drugs. For instance, it is plausible that compensated cirrhosis with thick septa, many small nodules and a large fibrosis area will be harder to treat and less likely to respond to therapies. Therefore, we have developed a machine learning model with 448 variables focusing on the key histological features of cirrhotic liver biopsies, including septa, nodules and fibrosis area. These variables correlated individually with HVPG measurements, and the correlation improved when they were combined into one score comprised of the most significant variables. The score assessed the CSPH with an excellent AUC of 0.85 in the training cohort and 0.74 in the validation cohort. Similarly, we created a score from the most significant variables to distinguish the presence of varices, which had an AUC of 0.86 in the training cohort and 0.73 in the validation cohort and a score to assess meaningful changes in HVPG, which had an AUC of 0.89. All these scores performed well and confirmed the value of including crucial histologic features of cirrhosis in histological assessment of liver biopsies. A recently published machine learning model which correlated well with CSPH in NASH cirrhosis patients included nodules of size that were weakly correlated with HVPG, and it did not consider septal thickness,[22] despite

previous literature demonstrating that septal thickness correlate with the severity of cirrhosis.[30] Also, the baseline machine learning HVPG score was not predictive of clinical liver events.

Our study has limitations and strengths. We were only able to correlate the ML model with HVPG, CSPH (and its changes) and the presence of varices. Further, there is a restriction of patient population due to the inclusion criteria of HVPG measurement >6 mmHg, and additional cohorts across a wider HVPG spectrum are needed confirm the generalisability of our findings. Recent studies have raised issues about the variabilities of HVPG measurement in NASH cirrhosis.[31] However, the HVPG measurements in this study[10] were made according to a rigorous protocol, including testing of the selected sites for qualification; using detailed measurement protocols; using balloons for wedge measurement; taking multiple reads; and using a central experienced HVPG reader.[13] In addition, the presence of varices is a valid measurement of portal hypertension for phase 2b NASH cirrhosis trials; other clinical liver events did not occur often enough in our study to be correlated with our ML model. The SNOF ML models would require evaluation in larger cohorts with longer follow-up to determine their prognostic utility in cirrhotic trials.

The study has many strengths as well: It was done in the setting of a randomised controlled trial with a central pathologist, endoscopist and portal pressure reader. All the readers were blinded to the treatment arm. Our sample size is the largest to date to assess this concept, using machine learning in a cohort with NASH cirrhosis. The SHG/TPE images technique uses unstained slides in comparison to other machine learning methods and thus may avoid traditional problems associated with staining liver tissue slides.[32]

In summary, we developed a histologic ML model that considers key histologic features in NASH cirrhosis: namely, septa, nodules and fibrosis area that have not been considered in the traditional histologic assessment. These features correlate with (HVPG) measurements and combining them with scores that correlated better with HVPG and clinically significant portal hypertension, distinguished the presence of varices and detected meaningful changes in HVPG. Our machine learning histology model offers a promising new method for NASH cirrhosis trials that may improve the assessment of histologic changes and drug efficacy.

5 | CONCLUSIONS

The machine learning algorithm accurately extrapolated hepatic venous pressure gradient, clinically significant portal hypertension and the development of varices from liver histology in patients with NASH cirrhosis. The use of the machine learning histology model in NASH cirrhosis trials may improve the assessment of histologic changes and drug efficacy.

ACKNOWLEDGEMENTS

The authors thank the patients who participated in this study, as well as the investigators and the study coordinators.

AUTHOR CONTRIBUTIONS

Study design: Mazen Noureddin, Zachary Goodman, Dean Tai, Naga Chalasani, Stephen A. Harrison, Harold Shlevin, and Pol Boudes. *Study conduct*: All authors. *Preparation of the manuscript*: Mazen Noureddin, Dean Tai, Yayun Ren, and Elaine Chng. *Critical review of the manuscript*: All authors. All authors approved the final version of the manuscript.

Mazen Noureddin: Conceptualization (equal); data curation (equal); funding acquisition (equal); investigation (equal); methodology (equal); project administration (equal); resources (equal); supervision (equal); validation (equal); visualization (equal); writing – original draft (equal); writing – review and editing (equal). **Zachary Goodman:** Conceptualization (equal); investigation (equal); methodology (equal); resources (equal); supervision (equal); validation (equal); writing – review and editing (equal). **Dean Tai:** Conceptualization (equal); formal analysis (equal); investigation (equal); methodology (equal); project administration (equal); resources (equal); software (equal); supervision (equal); validation (equal); visualization (equal); writing – original draft (equal); writing – review and editing (equal). **Elaine Chng:** Investigation (equal); methodology (equal); project administration (equal); resources (equal); supervision (equal); validation (equal); writing – original draft (equal); writing – review and editing (equal). **Ya Yun Ren:** Formal analysis (equal); investigation (equal); methodology (equal); resources (equal); software (equal); validation (equal); visualization (equal); writing – original draft (equal); writing – review and editing (equal). **Pol Boudes:** Conceptualization (equal); investigation (equal); methodology (equal); resources (equal); writing – review and editing (equal). **Harold Shlevin:** Conceptualization (equal); investigation (equal); methodology (equal); resources (equal); validation (equal); writing – review and editing (equal). **Guadalupe Garcia-Tsao:** Investigation (equal); project administration (equal); resources (equal); validation (equal); writing – review and editing (equal). **Stephen A. Harrison:** Conceptualization (equal); investigation (equal); methodology (equal); resources (equal); supervision (equal); validation (equal); writing – review and editing (equal). **Naga Chalasani:** Conceptualization (equal); investigation (equal); methodology (equal); resources (equal); supervision (equal); writing – review and editing (equal).

FUNDING INFORMATION

This study was funded by Galectin Therapeutics Inc.

CONFLICT OF INTEREST

These authors disclose the following: Mazen Noureddin has been on the advisory board for 89BIO, Altimmune, Gilead, cohBar, Cytodyn, Intercept, Pfizer, Novo Nordisk, Blade, EchoSens, Fractyl, Madrgial, Terns, Siemens and Roche diagnostic; has received research support from Allergan, BMS, Gilead, Galmed, Galectin, Genfit, Conatus, Enanta, Madrigal, Novartis, Pfizer, Shire, Viking and Zydus; and is a minor shareholder or has stocks in Anaetos, Rivus Pharma and Viking. Zachary Goodman receives research grant support from Gilead, Intercept, Galectin, Bristol-Myers Squibb, Novartis, Allergan, Conatus. Pol Boudes and Harold Shlevin are the

employees of Galectin Therapeutics, Inc. Guadalupe Garcia-Tsao has ongoing consulting activities with BioVie, Boehringer Ingelheim, Bristol-Myers Squibb, Conatus, Cook, Enterome, Galectin, Intercept and has received research grant support from Intercept. Stephen A. Harrison has provided consulting for Prometic, Innovate, CiVi, ContraVir, CymaBay, Echosens, Galectin, Galmed, Hightide, HistoIndex, Madrigal, Metacrine, NGM, Cirius, Perspectum, Akero, Terns, Viking, Blade, Poxel, Axcella, 3v Bio, Foresite, GENFIT, Intercept, Gilead, Novo Nordisk, Gelesis, Novartis, and NorthSea and has received research support from Pfizer, Novartis, Gilead, Bristol-Myers Squibb, ContraVir, CymaBay, Galectin, Galmed, Hightide, HistoIndex, Madrigal, Metacrine, NGM, Cirius, Akero, Axcella, 3v Bio, GENFIT, Intercept, Novo Nordisk, Novartis, Enyo, and NorthSea. Naga Chalasani has ongoing paid consulting activities with AbbVie, Madrigal, Foresite labs, Galectin, Zydus, Boehringer-Ingelheim, ObsEva, and Altimmune. He has grant support from Galectin, Exact Sciences and DSM. The remaining authors disclose no conflicts.

AUTHORSHIP

Guarantor of the article: Mazen Noureddin.

ORCID

Mazen Noureddin https://orcid.org/0000-0003-2127-2040
Guadalupe Garcia-Tsao https://orcid.org/0000-0001-8371-4524
Naga P. Chalasani https://orcid.org/0000-0003-4082-3178

REFERENCES

1. Setiawan VW, Stram DO, Porcel J, Lu SC, Le Marchand L, Noureddin M. Prevalence of chronic liver disease and cirrhosis by underlying cause in understudied ethnic groups: the multiethnic cohort. Hepatology. 2016;64:1969–77.
2. Noureddin M, Vipani A, Bresee C, Todo T, Kim IK, Alkhouri N, et al. NASH leading cause of liver transplant in women: updated analysis of indications for liver transplant and ethnic and gender variances. Am J Gastroenterol. 2018;113(11):1649–59.
3. Noureddin M, Anstee QM, Loomba R. Review article: emerging anti-fibrotic therapies in the treatment of non-alcoholic steatohepatitis. Aliment Pharmacol Ther. 2016;43(11):1109–23.
4. Vuppalanchi R, Noureddin M, Alkhouri N, Sanyal AJ. Therapeutic pipeline in nonalcoholic steatohepatitis. Nat Rev Gastroenterol Hepatol. 2021;18(6):373–92.
5. Al Attar A, Antaramian A, Noureddin M. Review of galectin-3 inhibitors in the treatment of nonalcoholic steatohepatitis. Expert Rev Clin Pharmacol. 2021;14(4):457–64.
6. Marcellin P, Gane E, Buti M, Afdhal N, Sievert W, Jacobson IM, et al. Regression of cirrhosis during treatment with tenofovir disoproxil fumarate for chronic hepatitis B: a 5-year open-label follow-up study. Lancet. 2013;381(9865):468–75.
7. Manne V, Akhtar E, Saab S. Cirrhosis regression in patients with viral hepatitis B and C: a systematic review. J Clin Gastroenterol. 2014;48(9):e76–84.
8. Noureddin M, Chan JL, Barradas K, Dimick-Santos L, Schabel E, Omokaro SO, et al. Attribution of nonalcoholic Steatohepatitis as an etiology of cirrhosis for clinical trials eligibility: recommendations from the multi-stakeholder liver forum. Gastroenterology. 2020;159(2):422–427 e421.
9. Anania FA, Dimick-Santos L, Mehta R, Toerner J, Beitz J. Nonalcoholic Steatohepatitis: current thinking from the division of Hepatology and nutrition at the Food and Drug Administration. Hepatology. 2021;73(5):2023–7.
10. Chalasani N, Abdelmalek MF, Garcia-Tsao G, Vuppalanchi R, Alkhouri N, Rinella M, et al. Effects of Belapectin, an inhibitor of galectin-3, in patients with nonalcoholic steatohepatitis with cirrhosis and portal hypertension. Gastroenterology. 2020;158(5):1334–1345, e1335.
11. Garcia-Tsao G, Bosch J, Kayali Z, Harrison SA, Abdelmalek MF, Lawitz E, et al. Randomized placebo-controlled trial of emricasan for non-alcoholic steatohepatitis-related cirrhosis with severe portal hypertension. J Hepatol. 2020;72(5):885–95.
12. Lens S, Rincon D, Garcia-Retortillo M, et al. Association between severe portal hypertension and risk of liver decompensation in patients with hepatitis C, regardless of response to antiviral therapy. Clin Gastroenterol Hepatol. 2015;13(10):1846–1853 e1841.
13. Garcia-Tsao G. Can we rely on changes in HVPG in patients with cirrhosis? Hepatology. 2021;74:2945–7.
14. Rinella ME, Tacke F, Sanyal AJ, Anstee QM, participants of the AEW. Report on the AASLD/EASL joint workshop on clinical trial endpoints in NAFLD. J Hepatol. 2019;71(4):823–33.
15. Sanyal AJ, Anstee QM, Trauner M, Lawitz EJ, Abdelmalek MF, Ding D, et al. Cirrhosis regression is associated with improved clinical outcomes in patients with nonalcoholic Steatohepatitis. Hepatology. 2021;75:1235–46.
16. Garcia-Tsao G, Friedman S, Iredale J, Pinzani M. Now there are many (stages) where before there was one: in search of a pathophysiological classification of cirrhosis. Hepatology. 2010;51(4):1445–9.
17. Nagula S, Jain D, Groszmann RJ, Garcia-Tsao G. Histological-hemodynamic correlation in cirrhosis—a histological classification of the severity of cirrhosis. J Hepatol. 2006;44(1):111–7.
18. Sethasine S, Jain D, Groszmann RJ, Garcia-Tsao G. Quantitative histological-hemodynamic correlations in cirrhosis. Hepatology. 2012;55(4):1146–53.
19. Kumar M, Sakhuja P, Kumar A, Manglik N, Choudhury A, Hissar S, et al. Histological subclassification of cirrhosis based on histological-haemodynamic correlation. Aliment Pharmacol Ther. 2008;27(9):771–9.
20. Dinani AM, Kowdley KV, Noureddin M. Application of artificial intelligence for diagnosis and risk stratification in NAFLD and NASH-the state of the art. Hepatology. 2021;74:2233–40.
21. Noureddin M. Artificial intelligence in NASH histology: human teaches a machine for the machine to help humans. Hepatology. 2021;74:9–11.
22. Bosch J, Chung C, Carrasco-Zevallos OM, Harrison SA, Abdelmalek MF, Shiffman ML, et al. A machine learning approach to liver histological evaluation predicts clinically significant portal hypertension in NASH cirrhosis. Hepatology. 2021;74:3146–60.
23. Liu F, Goh GB, Tiniakos D, Wee A, Leow WQ, Zhao JM, et al. qFIBS: an automated technique for quantitative evaluation of fibrosis, inflammation, ballooning, and steatosis in patients with nonalcoholic Steatohepatitis. Hepatology. 2020;71(6):1953–66.
24. Brunt EM, Janney CG, Di Bisceglie AM, Neuschwander-Tetri BA, Bacon BR. Nonalcoholic steatohepatitis: a proposal for grading and staging the histological lesions. Am J Gastroenterol. 1999;94(9):2467–74.
25. Kleiner DE, Brunt EM, Van Natta M, Behling C, Contos MJ, Cummings OW, et al. Design and validation of a histological scoring system for nonalcoholic fatty liver disease. Hepatology. 2005;41(6):1313–21.
26. Wang B, Sun Y, Zhou J, Wu X, Chen S, Wu S, et al. Advanced septa size quantitation determines the evaluation of histological fibrosis outcome in chronic hepatitis B patients. Mod Pathol. 2018;31(10):1567–77.
27. Popper H. Pathologic aspects of cirrhosis. A review. Am J Pathol. 1977;87(1):228–64.

28. Kearns M, Ron D. Algorithmic stability and sanity-check bounds for leave-one-out cross-validation. Neural Comput. 1999;11(6):1427–53.
29. Labenz C, Toenges G, Zheng MH, Ding D, Myers RP, Galle PR, et al. Derivation and validation of the nonalcoholic fatty liver disease cirrhosis score (NCS) to distinguish bridging fibrosis from cirrhosis. Eur J Intern Med. 2022;98:53–60.
30. Jain D, Sreenivasan P, Inayat I, Deng Y, Ciarleglio MM, Garcia-Tsao G. Thick fibrous septa on liver biopsy specimens predict the development of decompensation in patients with compensated cirrhosis. Am J Clin Pathol. 2021;156(5):802–9.
31. Bai W, Al-Karaghouli M, Stach J, Sung S, Matheson GJ, Abraldes JG. Test-retest reliability and consistency of HVPG and impact on trial design: a study in 289 patients from 20 randomized controlled trials. Hepatology. 2021;74:3301–15.
32. McGavin MD. Factors affecting visibility of a target tissue in histologic sections. Vet Pathol. 2014;51(1):9–27.

SUPPORTING INFORMATION

Additional supporting information will be found online in the Supporting Information section.

How to cite this article: Noureddin M, Goodman Z, Tai D, Chng ELK, Ren Y, Boudes P, et al. Machine learning liver histology scores correlate with portal hypertension assessments in nonalcoholic steatohepatitis cirrhosis. Aliment Pharmacol Ther. 2023;57:409–417. https://doi.org/10.1111/apt.17363